Supplemental material to this article can be found at:
http://dmd.aspetjournals.org/content/suppl/2018/04/03/dmd.118.080374.DC1

1521-009X/46/11/1572–1580$35.00
Drug Metabolism and Disposition
https://doi.org/10.1124/dmd.118.080374
Drug Metab Dispos 46:1572–1580, November 2018

Special Section – New Models in Drug Metabolism and Transport

Generation of Intestinal Organoids Suitable for Pharmacokinetic Studies from Human Induced Pluripotent Stem Cells[S]

Daichi Onozato, Misaki Yamashita, Anna Nakanishi, Takumi Akagawa, Yuriko Kida, Isamu Ogawa, Tadahiro Hashita, Takahiro Iwao, and Tamihide Matsunaga

Department of Clinical Pharmacy, Graduate School of Pharmaceutical Sciences (D.O., M.Y., A.N., T.H., T.I., T.M.), and Educational Research Center for Clinical Pharmacy, Faculty of Pharmaceutical Sciences (T.A., Y.K., I.O., T.H., T.I., T.M.), Nagoya City University, Nagoya, Japan

Received January 8, 2018; accepted March 29, 2018

ABSTRACT

Intestinal organoids morphologically resemble intestinal tissues and are expected to be used in both regenerative medicine and drug development studies, including pharmacokinetic studies. However, the pharmacokinetic properties of these organoids remain poorly characterized. In this study, we aimed to generate pharmacokinetically functional intestinal organoids from human induced pluripotent stem (iPS) cells. Human iPS cells were induced to differentiate into the midgut and then seeded on EZSPHERE plates (AGC Techno Glass Inc., Shizuoka, Japan) to generate uniform spheroids, and the floating spheroids were subsequently differentiated into intestinal organoids using small-molecule compounds. Exposure to the small-molecule compounds potently increased the expression of intestinal markers and pharmacokinetic-related genes in the organoids, and the organoids also included various intestinal cells such as enterocytes, intestinal stem cells, goblet cells, enteroendocrine cells, Paneth cells, smooth muscle cells, and fibroblasts. Moreover, microvilli and tight junctions were observed in the organoids. Furthermore, we detected not only the expression of drug transporters but also efflux transport activity through ABCB1/MDR1 and the induction of the drug-metabolizing enzyme CYP3A4 by ligands of nuclear receptors. Our results demonstrated the successful generation of pharmacokinetically functional intestinal organoids from human iPS cells. Thus, these intestinal organoids could be used as a pharmacokinetic evaluation system in drug development studies.

Introduction

The small intestine is a crucial organ for evaluating the pharmacokinetics of orally administered drugs, drug-metabolizing enzymes, including CYP3A4, and uptake and efflux transporters expressed in the small intestine (Zhang et al., 1999; Hilgendorf et al., 2007; Giacomini et al., 2010). CYP3A4 is involved in the metabolism of most drugs currently used in the clinic, and it is abundantly expressed in the small intestine (Paine et al., 2006). Thus, CYP3A4 plays an essential role in the first-pass metabolism of drugs (Kato, 2008). Moreover, CYP3A4 expression in the small intestine is known to be induced by rifampicin and 1α,25-dihydroxyvitamin D_3 (Thummel et al., 2001; Glaeser et al., 2005), and the induction of CYP3A4 expression in the small intestine causes a reduction in the bioavailability of orally administered drugs. Furthermore, the efflux transporter ABCB1/MDR1, which is highly expressed in the small intestine, functions as a barrier (Hilgendorf et al., 2007; Giacomini et al., 2010). Notably, in certain cases, substrates or inhibitors mediate interplay between CYP3A4 and ABCB1/MDR1, and thus intestinal pharmacokinetics must be assessed based on their contribution.

To accurately evaluate the pharmacokinetics in the human small intestine, human primary small intestinal cells or intestinal tissues must be used, but these cells and tissues are mostly unattainable in practice. Currently, Caco-2 cells, which are derived from a human colon

This study was supported by grants from the Japan Society for the Promotion of Science [Grants 26293036 and 16K15164]; the Research on Development of New Drugs from the Japan Agency for Medical Research and Development [Grants 15mk0101011h0102 and 17be0304203h0001]; the Japan Research Foundation for Clinical Pharmacology; and a Grant-in-Aid for Research in Nagoya City University in 2016.

The authors declare no conflict of interest.

https://doi.org/10.1124/dmd.118.080374.

[S]This article has supplemental material available at dmd.aspetjournals.org.

ABBREVIATIONS: A-83-01, 3-(6-methyl-2-pyridinyl)-*N*-phenyl-4-(4-quinolinyl)-1*H*-pyrazole-1-carbothioamide; 5-aza, 5-aza-2′-deoxycytidine; A/PD/5-aza, 3-(6-methyl-2-pyridinyl)-*N*-phenyl-4-(4-quinolinyl)-1*H*-pyrazole-1-carbothioamide (A-83-01), 2-(2-amino-3-methoxyphenyl)4*H*-1-benzopyran-4-one (PD98059), and 5-aza-2′-deoxycytidine (5-aza); BCRP, breast cancer resistance protein; CHIR99021, 6-[[2-[[4-(2,4-dichlorophenyl)-5-(5-methyl-1*H*-imidazol-2-yl)-2-pyrimidinyl]amino]ethyl]amino]-3-pyridinecarbonitrile; DAPT, *N*-[(3,5-difluorophenyl) acetyl]-L-alanyl-2-phenyl-1,1-dimethylethyl ester-glycine; DMEM/F12, Dulbecco's modified Eagle's medium and Ham's nutrient mixture F-12; FBS, fetal bovine serum; FD-4, fluorescein isothiocyanate-dextran 4000; FGF, fibroblast growth factor; HBSS, Hanks' balanced salt solution; iPS, induced pluripotent stem; L-Gln, L-glutamine; PCR, polymerase chain reaction; PD98059, 2-(2-amino-3-methoxyphenyl)4*H*-1-benzopyran-4-one; PXR, pregnane X receptor; UPLC, ultraperformance liquid chromatography; VDR, vitamin D receptor.

adenocarcinoma cell line and form polarized monolayers, are widely used in intestinal drug-absorption studies. However, in Caco-2 cells, the expression of transporters is distinct from that in normal intestinal cells, and the expression of drug-metabolizing enzymes is low (Nakamura et al., 2002; Sun et al., 2002; Borlak and Zwadlo, 2003). Moreover, CYP3A4 mRNA expression was reported to be induced by 1α,25-dihydroxyvitamin D_3 but not rifampicin in Caco-2 cells (Martin et al., 2008), but in a human in vivo study, intestinal CYP3A4 mRNA expression and activity were found to be induced after oral administration of rifampicin (Glaeser et al., 2005). Therefore, it might be challenging to accurately evaluate human intestinal pharmacokinetics using the Caco-2 cell monolayer model.

Intestinal cell monolayers lack organ-specific microarchitecture and a physiologic extracellular matrix microenvironment, which are critical for the self-renewal and maintenance of intestinal cells (Eglen and Randle, 2015). Recently, intestinal organoids, which are three-dimensional tissue structures, have attracted considerable attention in intestinal studies because these organoids structurally resemble intestinal tissues (Sato et al., 2009, 2011). Moreover, in the case of intestinal organoids derived from human induced pluripotent stem (iPS) cells, the organoids are composed of not only intestinal epithelial cells but also various intestinal cells such as intestinal stem cells and mesenchymal cells (McCracken et al., 2011; Spence et al., 2011; Watson et al., 2014; Finkbeiner et al., 2015; Tamminen et al., 2015). Thus, these organoids are expected to be useful in drug-development studies, such as drug screening and pharmacokinetic and toxicological evaluations (Eglen and Randle, 2015; Gould et al., 2015; Liu et al., 2016). In terms of pharmacokinetic functions, intestinal organoids generated from murine intestinal cells were successfully used for evaluating the function of the efflux transporter ABCB1/MDR1 (Mizutani et al., 2012; Zhang et al., 2016). However, to our knowledge, no report has been published on other pharmacokinetic properties of these organoids, such as their expression of drug-metabolizing enzymes and other transporters.

In this study, we aimed to establish the differentiation of human iPS cells into pharmacokinetically functional intestinal organoids. To induce highly effective differentiation, we modified a previous differentiation method (Spence et al., 2011) by using small-molecule compounds. We demonstrated that the differentiated intestinal organoids exhibited CYP3A4 activity and inducibility as well as efflux transporter activity of ABCB1/MDR1. We also identified small-molecule compounds that effectively induced intestinal differentiation. Our results indicate that human iPS cell–derived intestinal organoids can serve as a useful in vitro experimental system in pharmacokinetic studies.

Materials and Methods

Materials. The following materials were obtained from commercial sources: fibroblast growth factor (FGF) 2 and activin A, PeproTech Inc. (Rocky Hill, NJ); Matrigel Matrix Growth Factor Reduced (hereinafter referred to as Matrigel) and 40-μm nylon-mesh cell strainer, BD Biosciences Co. (Bedford, MA); 6-[[2-[[4-(2,4-dichlorophenyl)-5-(5-methyl-1*H*-imidazol-2-yl)-2-pyrimidinyl]amino]-ethyl]amino]-3-pyridinecarbonitrile (CHIR99021) and (+)-(*R*)-trans-4-(1-aminoethyl)-*N*-(4-pyridyl) cyclohexanecarboxamide dihydrochloride (Y-27632), Focus Biomolecules (Plymouth Meeting, PA); FGF4, BioLegend (San Diego, CA); EZSPHERE (microwell type #900: microwell size: diameter 500 μm, depth 100 μm), AGC Techno Glass Inc. (Shizuoka, Japan); KnockOut Serum Replacement, Advanced Dulbecco's modified Eagle's medium and Ham's nutrient mixture F-12 (DMEM/F12), N2 supplement, B27 serum-free supplement, and SlowFade Diamond Antifade Mountant, Thermo Fischer Scientific Inc. (Waltham, MA); fetal bovine serum (FBS), Nichirei Biosciences Inc. (Tokyo, Japan); R-spondin 1, noggin, and epidermal growth factor, GenScript (Piscataway, NJ); StemSure hPSC medium, verapamil, rifampicin, and 1α,25-dihydroxyvitamin D_3, Wako Pure Chemical Industries (Osaka, Japan); 2-(2-amino-3-methoxyphenyl)4-*H*-1-benzopyran-4-one (PD98059) and 3-(6-methyl-2-pyridinyl)-*N*-phenyl-4-(4-quinolinyl)-1*H*-pyrazole-1-carbothioamide (A-83-01), AdooQ BIOSCIENCE (Irvine, CA); 5-aza-2′-deoxycytidine (5-aza), Chem-Impex International, Inc. (Wood Dale, IL); *N*-[(3,5-difluorophenyl) acetyl]-L-alanyl-2-phenyl-1,1-dimethylethyl ester-glycine (DAPT), Peptide Institute Inc. (Osaka, Japan); O.C.T. Compound, Sakura Finetech Japan Co., Ltd. (Tokyo, Japan); fluorescein isothiocyanate-dextran 4000 (FD-4), Sigma-Aldrich (St. Louis, MO); rhodamine123, Takara Bio Inc. (Shiga, Japan); total RNA from human small intestine samples (five donors), BioChain Institute Inc. (Newark, CA); and all other reagents, which were of the highest quality available.

Maintenance of Human iPS Cells. A human iPS cell line (Windy) was provided by Dr. Akihiro Umezawa (National Center for Child Health and Development, Tokyo, Japan). Undifferentiated human iPS cells were maintained in DMEM/F12 supplemented with 5 ng/ml FGF2, 20% KnockOut Serum Replacement, 2 mM L-glutamine (L-Gln), 0.8% nonessential amino acids, and 0.1 mM 2-mercaptoethanol at 37°C in humidified air with 5% CO_2. The human iPS cells were cultured on a feeder layer of mitomycin C–treated murine embryonic fibroblasts, and the medium was changed daily.

Human iPS Cell Differentiation into Intestinal Organoids. Human iPS cells were passaged onto Matrigel-coated plates and cultured with StemSure hPSC medium supplemented with 35 ng/ml FGF2 before differentiation. After the cells reached 80% confluence, they were cultured with Roswell Park Memorial Institute 1640 medium supplemented with FBS, 2 mM L-Gln, 100 U/ml penicillin, 100 μg/ml streptomycin, and 100 ng/ml activin A for 3 days. The FBS concentration was gradually increased from 0% to 0.2% or 2%. Subsequently, the medium was replaced with Roswell Park Memorial Institute 1640 medium containing 2 mM GlutaMAX, 2% FBS, 3 μM 6-[[2-[[4-(2,4-dichlorophenyl)-5-(5-methyl-1*H*-imidazol-2-yl)-2-pyrimidinyl]amino]ethyl]amino]-3-pyridinecarbonitrile, and 500 ng/ml FGF4, and then the cells were trypsinized for 3 minutes and filtered through a 40-μm nylon-mesh cell strainer. Next, the cells (4.0×10^6 cells) were seeded onto EZSPHERE plates to generate spheroids and cultured with 10 μM (+)-(*R*)-trans-4-(1-aminoethyl)-*N*-(4-pyridyl) cyclohexanecarboxamide dihydrochloride for 72 hours, after which the spheroids were transferred to ultralow attachment plates, and after the passage cultured with Advanced DMEM/F12 containing 3% Matrigel, 200 ng/ml R-spondin1, 100 ng/ml noggin, 100 ng/ml epidermal growth factor, 2 mM L-Gln, 15 mM HEPES, N2 supplement, B27 serum-free supplement, 100 U/ml penicillin, and 100 μg/ml streptomycin for 27 days. On days 19–34, 0.5 μM A-83-01, 20 μM PD98059, 5 μM 5-aza, and 5 μM DAPT were added. The medium was changed every 3 days. In the induction study, 40 μM rifampicin or 1 μM 1α,25-dihydroxyvitamin D_3 was added in the medium for the final 72 hours.

RNA Extraction, Reverse Transcription Reaction, and Real-Time Polymerase Chain Reaction (PCR) Analysis. Total RNA was isolated from human iPS cell–derived intestinal organoids using the Agencourt RNAdvance Tissue Kit (Beckman Coulter Inc., Brea, CA). First-strand cDNA was prepared from 1 μg of total RNA. The reverse-transcription reaction was performed using the ReverTra Ace qPCR RT Master Mix (TOYOBO, Shiga, Japan), according to the manufacturer's instructions. Real-time PCR analysis was performed on an Eco Real-Time PCR System using Eco Real-Time PCR System software version 5.0 (Illumina Inc., San Diego, CA). PCR was performed with the primer pairs listed in Table 1 using a KAPA SYBR Fast qPCR Kit (NIPPON Genetics Co., Tokyo, Japan). All mRNA expression levels were normalized relative to that of the housekeeping gene encoding HPRT.

H&E and Alcian Blue Staining. After differentiation, intestinal organoids were fixed with 4% paraformaldehyde, frozen, embedded in O.C.T. Compound, and then cut into 10-μm sections. H&E staining was performed according to the conventional method. For alcian blue staining, alcian blue at pH 2.5 was used, and nuclei were stained with Nuclear Fast Red.

Immunofluorescence Staining. From differentiated organoids, 10-μm frozen sections were prepared as described in the preceding subsection and attached to glass slides. Antigen retrieval was performed with 10 mM citrate buffer (pH 8.0) in a microwave oven. After blocking in phosphate-buffered saline containing 5% FBS for 30 minutes, sections were reacted with the primary antibodies at 4°C overnight, washed, and then incubated with secondary antibodies at room temperature for 1 hour. Nuclei were stained with 4′,6-diamidino-2-phenylindole. The antibodies used and their dilutions are shown in Table 2. Finally, sections were washed and mounted using SlowFade Diamond Antifade Mountant, and confocal images were captured and analyzed using a Zeiss LSM510 microscope and AxioVision software (Carl Zeiss, Oberkochen, Germany).

Transmission Electron Microscopy. Human iPS cell–derived intestinal organoids were fixed with 2.5% glutaraldehyde overnight at 4°C and then postfixed

TABLE 1

Primers used for real-time PCR analysis

Gene Name	Sense (5′→3′)	Antisense (5′→3′)	Product Length
			bp
ABCB1/MDR1	CCCATCATTGCAATAGCAGG	TGTTCAAACTTCTGCTCCTGA	158
ABCC2/MRP2	ACAGAGGCTGGCAACC	ACCATTACCTTGTCCATCA	227
ABCC3/MRP3	GTCCGCAGAATGGACTTGAT	TCACCACTTGGGGATCATTT	120
ABCG2/BCRP	AGATGGGTTTCCAAGCGTTCAT	CCAGTCCCAGTACGACTGTGACA	91
CDX2	ACCTGTGCGAGTGGATGC	TCCTTTGCTCTGCGGTTCT	232
Chromogranin A	TCCGACACACTTTCCAAGCC	TTCTGCTGATGTGCCCTCTC	164
CYP2C9	GACATGAACAACCCTCAGGACTTT	TGCTTGTCGTCTCTGTCCCA	145
CYP2C19	GAACACCAAGAATCGATGGACA	TCAGCAGGAGAAGGAGAGCATA	196
CYP2D6	CCTACGCTTCCAAAAGGCTTTT	AGAGAACAGGTCAGCCACCACT	178
CYP3A4	CTGTGTGTTTCCAAGAGAAGTTAC	TGCATCAATTTCCTCCTGCAG	298
HPRT	CTTTGCTTTCCTTGGTCAGG	TCAAGGGCATATCCTACAACA	148
LGR5	TGCTCTTCACCAACTGCATC	CTCAGGCTCACCAGATCCTC	193
Lysozyme	TCAATAGCCGCTACTGGTGT	AATGCCTTGTGGATCACGGA	143
MUC2	AGAAGGCACCGTATATGACGAC	CAGCGTTACAGACACACTGCTC	137
PXR	AGGATGGCAGTGTCTGGAAC	AGGGAGATCTGGTCCTCGAT	174
SLC10A2/ASBT	ATGCAGAACACGCAGCTATG	GCTCCGTTCCATTTTCTTTG	205
SLC15A1/PEPT1	CACCTCCTTGAAGAAGATGGCA	GGGAAGACTGGAAGAGTTTTATCG	105
SLC16A1/MCT1	TCATGTATGGTGGAGGTCCTAAC	ACCTCCAATGACTCCAATACAGA	161
SLC22A1/OCT1	TAATGGACCACATCGCTCAA	AGCCCTGATAGAGCACAGA	190
SLC51A/OSTA	GCCCTACAGCCCCTCCATC	TGAGGAGGTGGCAATTCA	109
SLCO1A2/OATP1A2	TGCATTCGTTAACATGATCTCC	CCTATGTGGGCAGCTTGTTT	183
SLCO2B1/OATP2B1	CTTCATCTCGGAGCCATACC	GCTTGAGCAGTTGCCATTG	130
VDR	CTCTTCAGACATGATGGACTCG	GGATGCTGTAACTGACCAGG	140
Villin	AGCCAGATCACTGCTGAGGT	TGGACAGGTGTTCCTCCTTC	169

bp, base pair.

with 1% osmium tetroxide for 2 hours at 4°C. Next, the samples were dehydrated with ethanol and embedded in resin, and the embedded samples were cut into 0.1-μm sections. The sections were stained with uranyl acetate and examined using a Hitachi H7600 transmission electron microscope (JEOL, Tokyo, Japan).

FD-4 Permeability Study. Human iPS cell–derived intestinal organoids were washed with Hanks' balanced salt solution [(HBSS), pH 7.4)] and incubated with HBSS containing 1 mg/ml FD-4 for 1 hour at 37°C. After incubation, the organoids were washed with ice-cold HBSS and then examined using an ECLIPSE Ti-S microscope (Nikon, Tokyo, Japan).

Efflux Transport Analysis. Human iPS cell–derived intestinal organoids were rinsed several times with phosphate-buffered saline and incubated with HBSS containing 10 μM rhodamine123 for 1 hour at 37°C with or without 100 μM verapamil. After incubation, the organoids were washed with ice-cold HBSS and examined using a Zeiss LSM510 microscope and AxioVision software (Carl Zeiss). In transport analysis, via breast cancer resistance protein (BCRP), hoechst33342 (10 μM) and Ko143 (100 μM) were used as the substrate and inhibitor, respectively. The analysis was performed using the same method described previously.

Determination of CYP3A4 Activity. Intestinal organoids were incubated with Advanced DMEM/F12 containing 2 mM L-Gln, N2 supplement, B27 serum-free supplement, 100 U/ml penicillin, 100 μg/ml streptomycin, and 15 mM HEPES containing 50 μM midazolam for 24 hours at 37°C. After incubation, 100 μl of the reaction medium was collected, and the reaction was stopped by adding 200 μl of ice-cold acetonitrile containing 3.6 μM chlorpropamide as an internal standard. The levels of 1′-hydroxylated metabolites in the mixture were measured using ultraperformance liquid chromatography (UPLC)/tandem mass spectrometry. For UPLC/tandem mass spectrometry analyses, samples were thawed and centrifuged at 20,600*g* for 5 minutes at room temperature. To measure metabolites, 10-μl aliquots of the supernatant were injected into the UPLC/tandem mass spectrometry apparatus. UPLC analysis was performed using an ACQUITY UPLC system (Waters, Milford, MA) equipped with an XBridge BEH

TABLE 2

Primary and secondary antibodies

Antibody Name	Source	Catalog Number	Biologic Source	Dilution
α-Smooth muscle actin	Abcam	ab5694	Rabbit	1:200
ABCB1/MDR1	GeneTex	GTX23364	Mouse	1:50
ABCG2/BCRP	Abcam	ab3380	Mouse	1:100
Chromogranin A	IMMUNOSTAR	20085	Rabbit	1:500
CDX2	BioGenex	MU392A-UC	Mouse	1:100
E-Cadherin	BD Transduction Laboratories	610181	Mouse	1:100
Ki67	eBioscience	14-5699	Mouse	1:100
LGR5	ABGENT	AP2745d	Rabbit	1:100
Lysozyme	BioGenex	AR024-5R	Rabbit	–
MUC2	Santa Cruz	sc-15334	Rabbit	1:200
Occludin	Thermo Fisher Scientific	71-1500	Rabbit	1:100
Olfactomedin 4	Abcam	ab85046	Rabbit	1:100
SLC15A1/PEPT1	Santa Cruz	sc-20654	Rabbit	1:100
Villin	Santa Cruz	sc58897	Mouse	1:100
Vimentin	Abcam	ab8069	Mouse	1:200
Alexa Fluor 488 donkey anti-Rabbit IgG (H&L)	Thermo Fisher Scientific	A-21206	Rabbit	1:200
Alexa Fluor 488 goat anti-Mouse IgG (H&L)	Thermo Fisher Scientific	A-11001	Mouse	1:200
Alexa Fluor 568 goat anti-Mouse IgG (H&L)	Thermo Fisher Scientific	A-11004	Mouse	1:200

—: Anti-Lysozyme antibody was used without dilution.

C18 column (2.1 × 50 mm, 3.5 μm; Waters). The mobile phase consisted of 10 mM ammonium formate (A) and acetonitrile (B), and the column and sample temperatures were 40°C and 4°C, respectively. A gradient containing 5% B was started at the flow rate of 0.25 ml/min, and 0.5 minutes later the gradient was increased linearly for 2.0 minutes until 95% B. Subsequently, the flow rate was raised to 0.55 ml/min by 2.1 minutes, and the gradient was maintained at 95% B until 3.5 minutes. Finally, the gradient was linearly decreased to 5% B by 3.6 minutes, and the flow rate was decreased to 0.25 ml/min by 3.7 minutes, which was maintained until 5.4 minutes. Multiple reactions monitoring was used for detection of 1′-hydroxy midazolam derivatives (*m/z* 342.03 → 168.40). Chromatographic data were analyzed using Mass Lynx 4.1 software (Waters). The organoids were solubilized with 1 M NaOH, and lysates were collected. To correct for CYP3A4 activity, the total protein content was measured using a Pierce BCA Protein Assay Kit (Takara Bio Inc.), according to the manufacturer's instructions.

Statistical Analysis. For experiments involving human iPS cell–derived intestinal organoids, *n* represents the number of biologic replicates (three-to-four

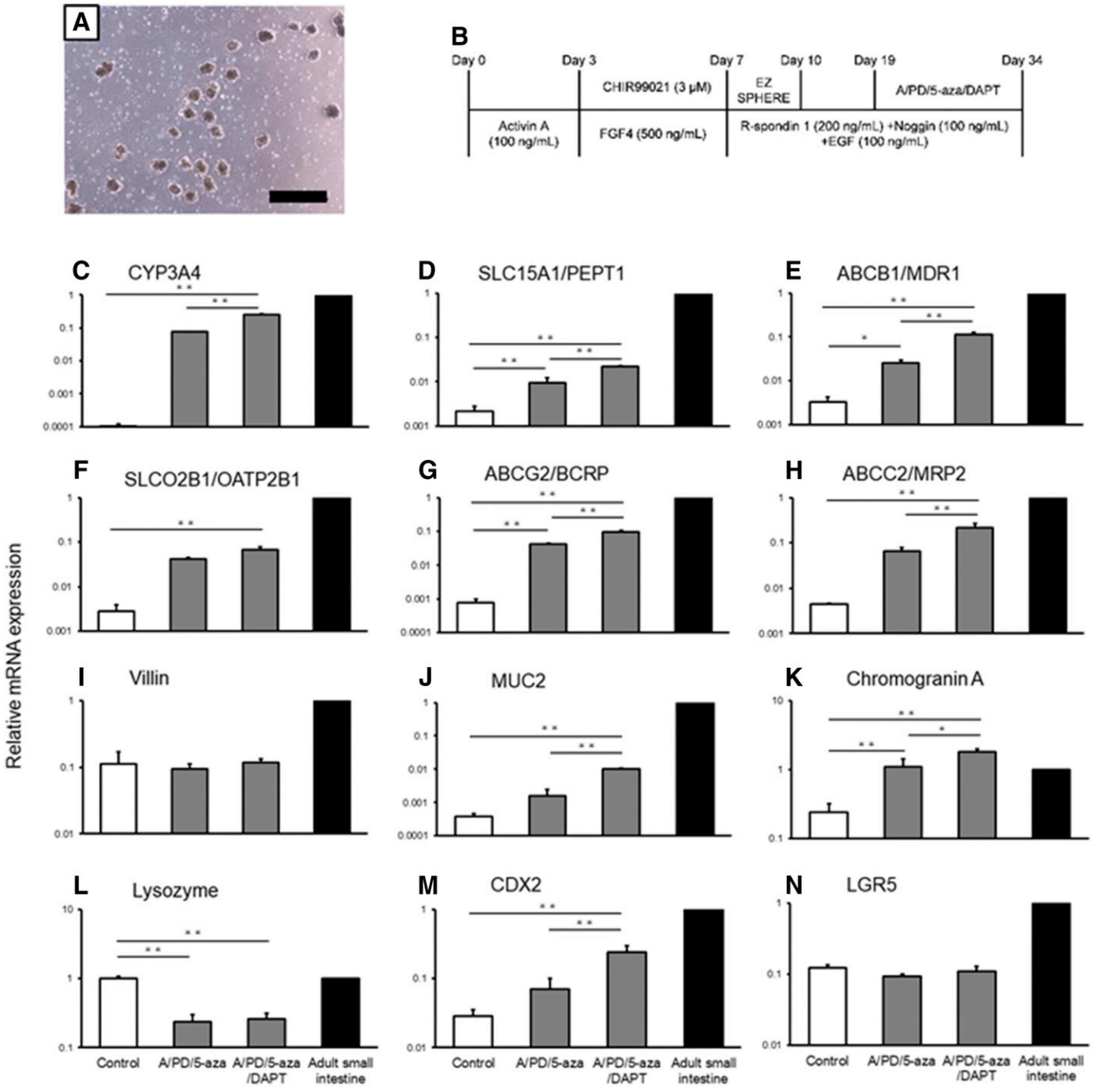

Fig. 1. Generation of intestinal organoids from human iPS cells and effects of small-molecule compounds on differentiation to intestinal organoids. (A) Image of uniform spheroids in suspension culture on day 10. Scale bar, 500 μm. (B) Protocol of intestinal organoid differentiation. (C–N) mRNA expression of pharmacokinetic-related genes and intestinal markers in human iPS cell–derived intestinal organoids. Human iPS cells were cultured in the presence of activin A for 3 days. The cells were further cultured in medium containing 6-[[2-[[4-(2,4-dichlorophenyl)-5-(5-methyl-1*H*-imidazol-2-yl)-2-pyrimidinyl]amino]ethyl]amino]-3-pyridinecarbonitrile (CHIR99021) and FGF4 for 4 days and then in the presence of 3% Matrigel, R-spondin1, noggin, and epidermal growth factor (EGF) for 27 days in suspension culture. A/PD/5-aza or A/PD/5-aza/DAPT was added on days 19–34. After 34 days of differentiation, total RNA was extracted, and mRNAs were analyzed using SYBR Green real-time PCR. Data are represented as mean ± S.D. ($n = 3$). All mRNA expression levels were normalized relative to the mRNA level of HPRT. Gene expression levels are represented relative to the level in the adult small intestine, which was set to 1. Statistical analysis was performed using Bonferroni's correction: $^*P < 0.05$; $^{**}P < 0.01$.

wells were collected for each replicate). Each experiment was repeated on at least two separate occasions (independent experiments). Quantified data are represented as mean ± S.D. Statistical comparisons between groups were performed using two-tailed Student's *t* test (Fig. 6A), one-way analysis of variance with Bonferroni's correction (Fig. 1), or two-tailed Dunnett's test by PASW Statistics 18 software (IBM, Chicago, IL) (Fig. 6, B and C). Significant differences are indicated by *P* values listed in the Figs. 1C–N and 6.

Results

Differentiation into Intestinal Organoids. To generate a large quantity of uniformly sized spheroids efficiently and simply, human iPS cell–derived midguts were seeded on EZSPHERE plates. The size of the spheroids was uniform after culture on the plates for 3 days (Fig. 1A). Next, we generated intestinal organoids from the spheroids using A-83-01, PD98059, and 5-aza (A/PD/5-aza) or A/PD/5-aza plus DAPT (Fig. 1B). Relative to the control group, the groups treated with the small-molecule compounds—particularly A/PD/5-aza/DAPT—showed significantly increased mRNA expression levels of these pharmacokinetic-related genes (Fig. 1, C–H): CYP3A4, SLC15A1/-PEPT1, SLCO2B1/OATP2B1, ABCC2/MRP2, ABCG2/BCRP, and ABCB1/MDR1. These proteins are drug-metabolizing enzymes and drug transporters expressed in the small intestine (Zhang et al., 1999; Hilgendorf et al., 2007; Giacomini et al., 2010). Using quantitative PCR analysis, we also measured expression levels of other pharmacokinetic-related genes such as CYP2C9, CYP2C19, CYP2D6, SLC10A2/ASBT, SLC16A1/MCT1, ABCC3/MRP3, SLCO1A2/OATP1A2, SLC22A1/OCT1, SLC51A/OSTA, pregnane X receptor (PXR), and vitamin D receptor (VDR). The expression levels of these genes, except SLC10A2/ASBT, were higher than in the small intestine (Supplemental Fig. 1). In particular, the expression of SLCO1A2/OATP1A2, which is expressed from the duodenum to jejunum, was markedly higher than that of human adult intestine; on the other hand, expression of SLC10A2/ASBT, which is expressed in the ileum, was considerably lower than that of human adult intestine. In addition, the mRNA expression levels of PXR and VDR were low compared with those in adult small intestine. Treatment with A/PD/5-aza/DAPT also resulted in a significant increase in the mRNA levels of MUC2 (Reis et al., 1999), chromogranin A (Cetin et al., 1989; Sato et al., 2003), and CDX2 (Boudreau et al., 2002), which are, respectively, goblet cell, enteroendocrine, and hindgut markers (Fig. 1, J, K, and M). By contrast, the mRNA expression of lysozyme, a Paneth cell marker (Peeters and Vantrappen, 1975), was decreased after the treatment, and the mRNA expression levels were almost the same among the groups in the case of LGR5, an intestinal stem cell marker (Barker et al., 2007), and villin, an enterocyte marker (Robine et al., 1985) (Fig. 1, I, L, and N). Based on these results, treatment with A/PD/5-aza/DAPT was considered the most effective among the tested treatments, and thus, in the following experiments, we used the organoids that were induced to differentiate using A/PD/5-aza/DAPT.

Human iPS cell–derived intestinal organoids that were differentiated by adding A/PD/5-aza/DAPT formed highly uniform bubble-like structures (Fig. 2A). H&E staining results showed that the organoids consisted of a mucosa and submucosa (Fig. 2B), and alcian blue staining further revealed mucus production in the epithelium of the intestinal organoids (Fig. 2C). Moreover, microvilli, tight junctions, secretory granules, and mucin granules were observed in the organoids in transmission electron microscopy analysis (Fig. 2, D–F).

In other assays, immunofluorescence staining showed that human iPS cell–derived intestinal organoids expressed villin, olfactomedin 4, and LGR5 (intestinal stem cell markers); Ki67 (proliferation marker);

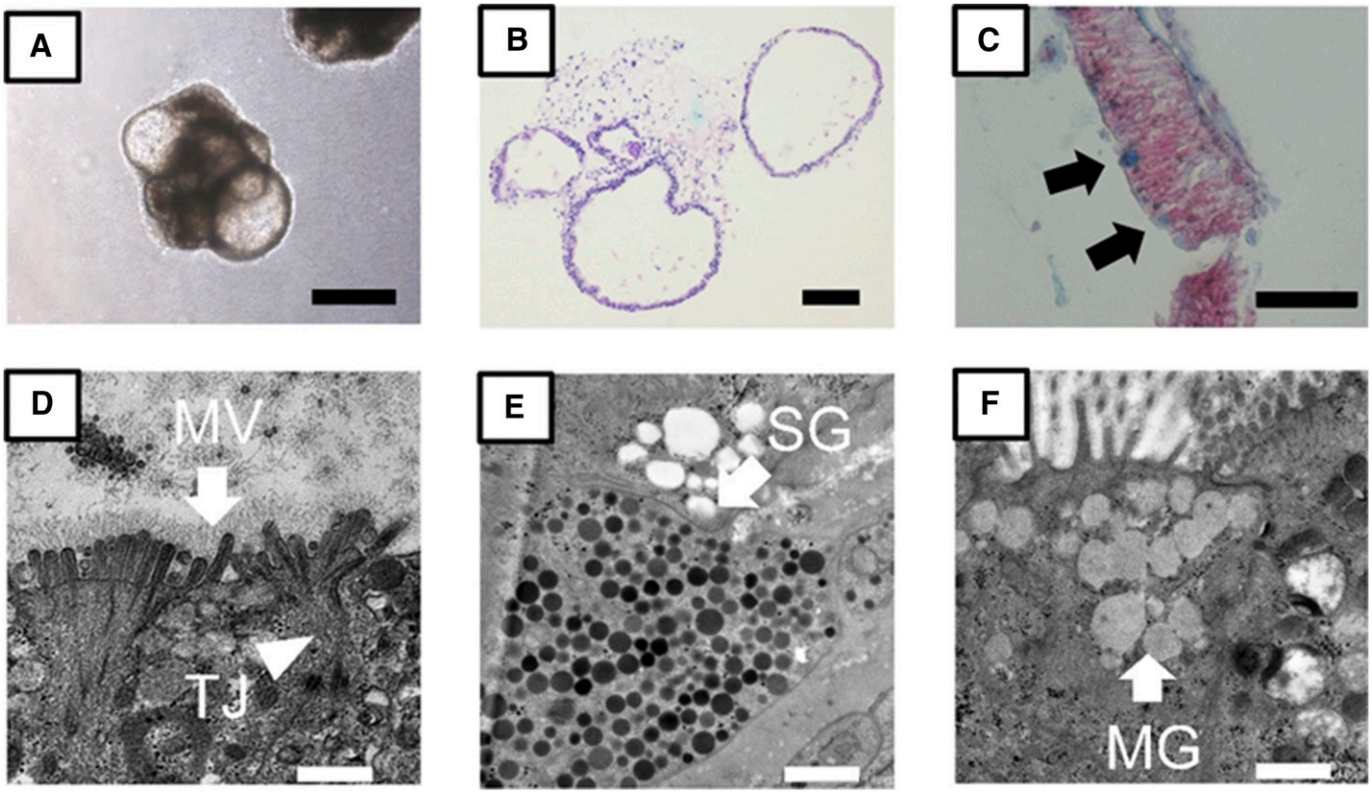

Fig. 2. Morphology of human iPS cell–derived intestinal organoids. (A) Phase-contrast microscopy image. Scale bar, 500 μm. (B) H&E staining. Scale bar, 100 μm. (C) Alcian blue staining. Scale bar, 100 μm. Black arrows, alcian blue–positive cells. (D–F) Transmission electron microscopy images. (D) Microvilli (MV) white arrow, and tight junctions (TJ), white arrow head. (E) Secretory granules (SG), white arrow. (F) Mucin granules (MG), white arrow. Scale bar, 1 μm.

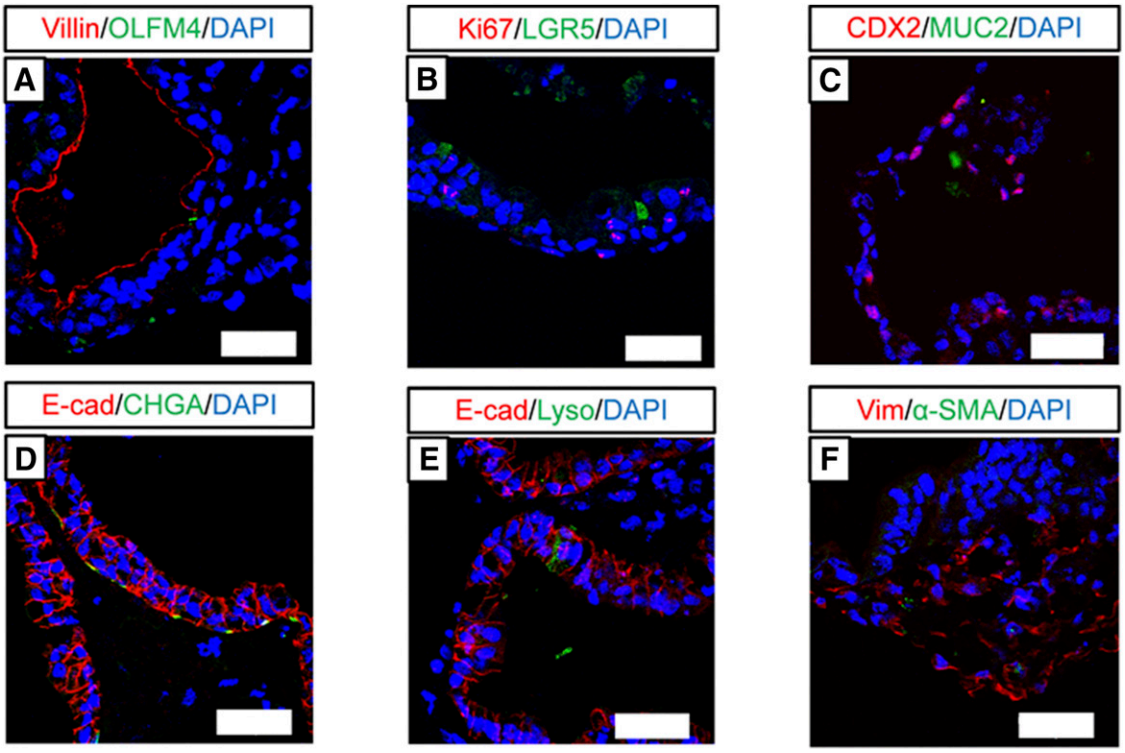

Fig. 3. Immunofluorescence staining of various intestinal cell markers in human iPS cell–derived intestinal organoids. (A–F) Images showing immunofluorescence staining for villin and olfactomedin 4 (OLFM4) (A), Ki67 and LGR5 (B), CDX2 and MUC2 (C), E-cadherin (E-cad) and chromogranin A (CHGA) (D), E-cad and lysozyme (Lyso) (E), and vimentin (Vim) and α-smooth muscle actin (α-SMA) (F). Scale bar, 50 μm. Nuclei were counterstained with 4′,6-diamidino-2-phenylindole (DAPI).

CDX2, MUC2, and E-cadherin (epithelial cell markers); chromogranin A, lysozyme, and vimentin (mesenchymal cell markers); and α-smooth muscle actin (Fig. 3).

Analysis of Functional Tight Junction and Drug Transporters. To investigate whether human iPS cell–derived intestinal organoids formed functional tight junctions, we performed immunofluorescence staining for occludin, which is a tight junction marker (González-Mariscal et al., 2003), and measured the permeability of FD-4. Occludin was expressed along the lumen of the intestinal organoids (Fig. 4A), and FD-4 did not permeate into the intestinal organoids (Fig. 4, B and C). We found that SLC15A1/PEPT1, ABCB1/MDR1, and ABCG2/BCRP were also expressed along the lumen of the intestinal organoids (Fig. 5, A–C). To assess the function of ABCB1/MDR1 and ABCG2/BCRP, we performed transport assays using rhodamine123 and hoechst33342, fluorescent dyes that are substrates of ABCB1/MDR1 and ABCG2/BCRP, respectively (Takano et al., 1998; Perloff et al., 2003). Efflux of rhodamine123 into the organoids was observed (Fig. 5, D and E), and this was inhibited by verapamil (Fig. 5, F and G), an inhibitor of ABCB1/MDR1 (Shirasaka et al., 2008). In addition, efflux of hoechst33342 into the organoids was observed, and this was inhibited by Ko143, an inhibitor of ABCG2/BCRP (Supplemental Fig. 2).

Activity and Inducibility of CYP3A4. We investigated whether CYP3A4 metabolic activity is induced in human iPS cell–derived intestinal organoids. The metabolic activity of CYP3A4 was evaluated using a specific substrate and inhibitor, midazolam and ketoconazole, respectively. Metabolic activity toward midazolam was detected in the organoids and was significantly inhibited by up to ~38% by ketoconazole (Fig. 6A). To test for CYP3A4 induction, we used rifampicin and 1α,25-dihydroxyvitamin D_3, which are ligands of PXR and VDR, respectively. The CYP3A4 mRNA expression level was approximately 2- and 4.5-fold higher following the addition of rifampicin and 1α,25-dihydroxyvitamin D_3, respectively (Fig. 6B). Moreover, CYP3A4 activity was induced roughly 1.5- and 2.0-fold by rifampicin and 1α,25-dihydroxyvitamin D_3, respectively (Fig. 6C).

Discussion

In this study, we successfully produced pharmacokinetically functional intestinal organoids from human iPS cells using A/PD/5-aza/DAPT. Generation of intestinal organoids derived from human iPS cells has been described in a few previous reports (McCracken et al., 2011; Spence et al., 2011; Finkbeiner et al., 2015; Tamminen et al., 2015). However, the methods used are complicated and time consuming,

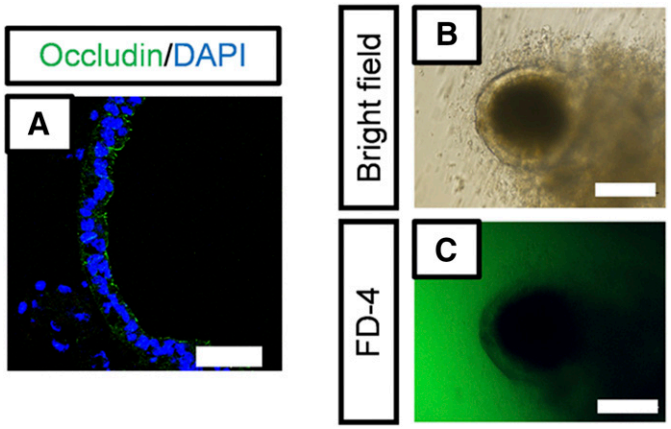

Fig. 4. Analysis of barrier function. (A) Immunofluorescence staining of tight junction marker occludin (green). Scale bar, 50 μm. Nuclei were counterstained with 4′,6-diamidino-2-phenylindole (DAPI) (blue). (B and C) FD-4 permeability in human iPS cell–derived intestinal organoids. Organoids were incubated with FD-4 (1 mg/ml) for 1 hour at 37°C. Bright-field image (B) and fluorescence image (C). Scale bar, 50 μm.

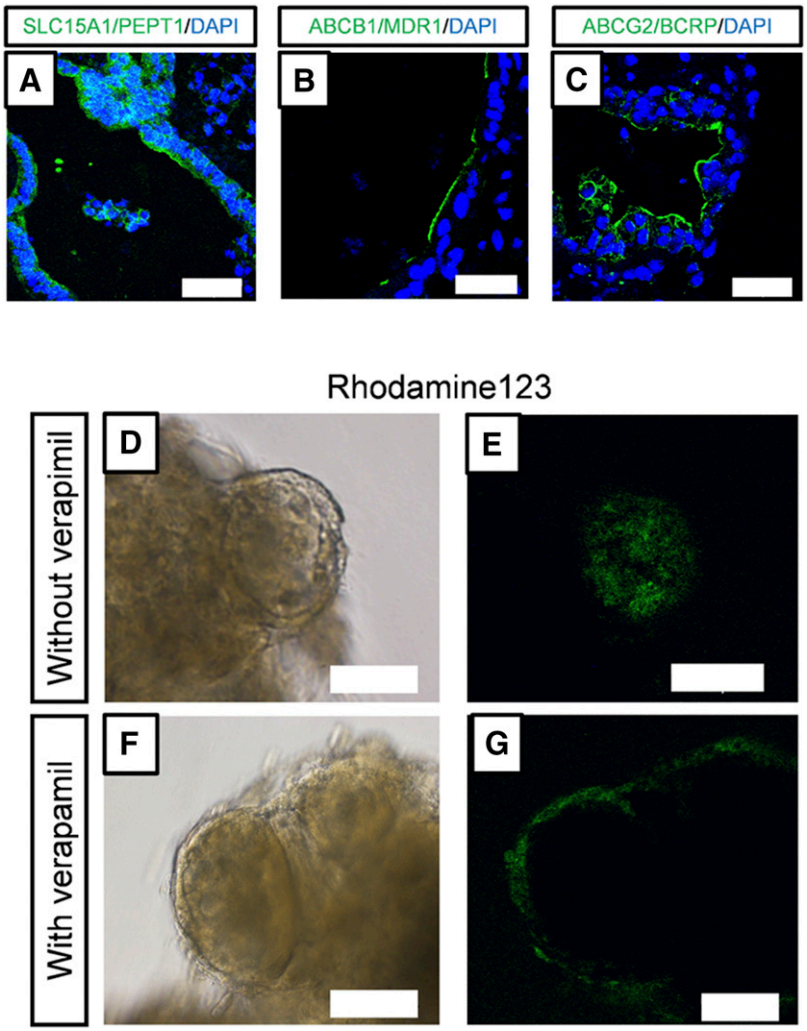

Fig. 5. The expression of drug transporters and efflux transport of rhodamine123. (A–C) Immunofluorescence staining of SLC15A1/PEPT1 (A, green), ABCB1/MDR1 (B, green), and ABCG2/BCRP (C, green). Scale bar, 50 μm. Nuclei were counterstained with 4′,6-diamidino-2-phenylindole (DAPI) (blue). (D–G) Efflux transport of rhodamine123 through ABCB1/MDR1. Organoids were incubated with rhodamine123 (10 μM) for 1 hour at 37°C in the absence (D and E) or presence (F and G) of verapamil (100 μM). Bright-field images (D and F). Fluorescence images (E and G). Scale bar, 100 μm.

and a large number of intestinal organoids could not be cultured. Here, we used EZSPHERE to generate uniform spheroids abundantly and subsequently performed a suspension culture, and this enabled us to readily and simply generate numerous uniform spheroids (Fig. 1B). We also succeeded in generating a floating culture to enable mass culture. With previous methods, such as the Matrigel-embedding method, the application to drug screening and high-throughput screening remained difficult because of culture scalability limitations; our protocols may allow application to these assays, which require large amounts of uniform intestinal organoids.

To promote intestinal differentiation, we next tested several compounds, which revealed that the mRNA expression of pharmacokinetic-related genes was markedly increased following treatment with A/PD/5-aza/DAPT (Fig. 1, C–H). In the A/PD/5-aza/DAPT treatment group, most genes were expressed almost at the same level as in the small intestine, and a notable increase was observed in the mRNA expression of various intestinal cell markers, such as MUC2, chromogranin A, and CDX2 (Fig. 1, J, K, and M). Conversely, expression of Paneth cell markers, such as lysozyme, was significantly decreased compared with the level in the nontreatment group, and the levels of the enterocyte marker villin and the intestinal stem cell marker LGR5 were unaltered (Fig. 1, I, L, and N). Our results suggest that these small-molecule compounds promoted the differentiation into intestinal epithelial cells, including secretory cells, rather than Paneth cells and intestinal stem cells. Previously, we reported that the combination of A-83-01, PD98059, and 5-aza induced the differentiation of human iPS cells into enterocyte-like cells (Iwao et al., 2015). Moreover, DAPT and a Wnt agonist were reported to stimulate the differentiation of human embryonic stem cells into intestinal epithelial cells (Ogaki et al., 2013). It has also been reported that DAPT blocks Notch activation, resulting in promotion of the maturation of intestinal epithelial cells or differentiation into secretory cells (Sander and Powell, 2004). On the other hand, the mRNA expression of lysozyme, a Paneth cell marker, was decreased after treatment with A/PD/5-aza or A/PD/5-aza/DAPT, suggesting that the differentiation into Paneth cells may be suppressed by treatment with these compounds. Based on these results, we suggest that these small-molecule compounds promote the differentiation of human iPS cell–derived intestinal organoids by exerting additive effects; however, further investigation of the detailed mechanism is required. In addition, the mRNA expression level of SLCO1A2/OATP1A2, which is expressed from the duodenum to jejunum, was markedly higher than that of human adult intestine; on the other hand, mRNA expression of SLC10A2/ASBT, which is expressed in the ileum, was considerably lower than that of human adult intestine (Supplemental Fig. 1, D and I). Therefore, the characteristics of the intestinal organoids may resemble those of the duodenum or jejunum.

In the intestinal organoids derived from human iPS cells, villin, occludin, SLC15A1/PEPT1, ABCB1/MDR1, and ABCG2/BCRP were localized along the lumen of the polarized columnar epithelium, and microvilli and tight junctions were present in the organoids (Figs. 2D, Figs. 3A, Figs.4A, and Figs. 5, A–C). These results suggested that the

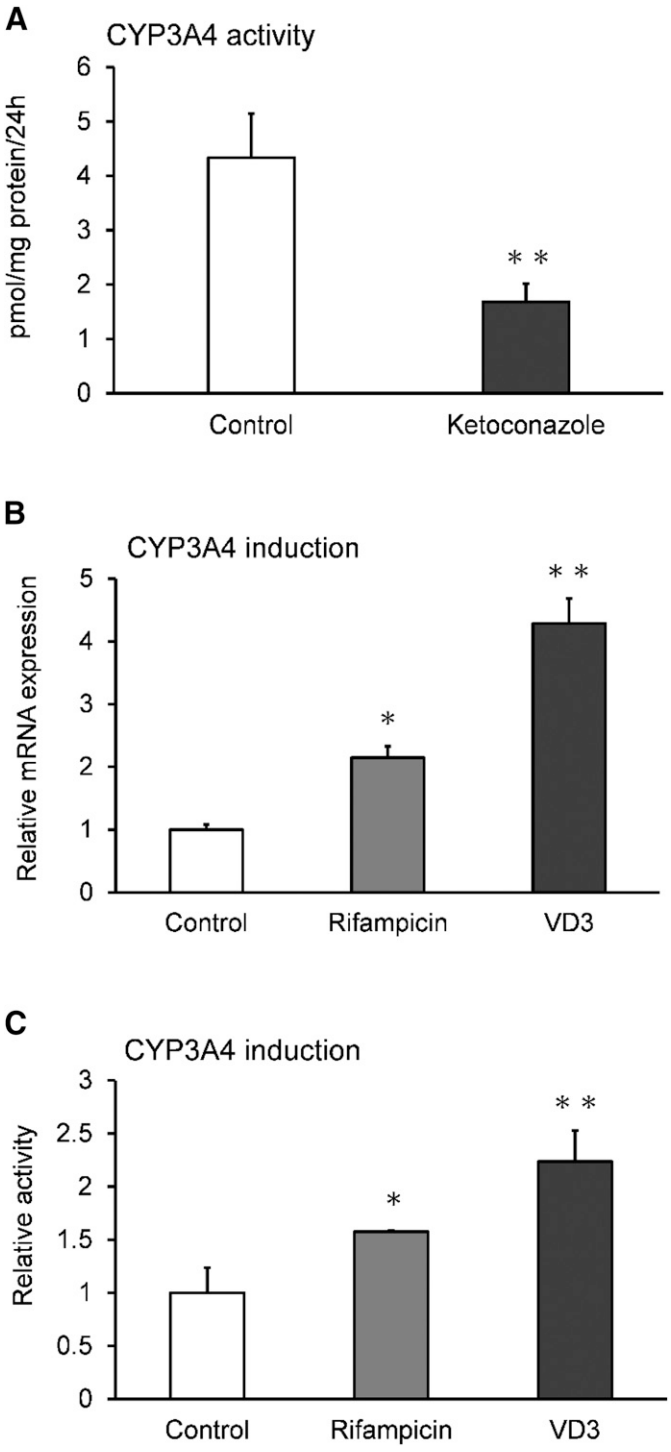

Fig. 6. Activity and inducibility of CYP3A4. (A) Metabolic activity of CYP3A4 in human iPS cell–derived intestinal organoids. Data are represented as mean ± S.D. (n = 4). Differences relative to the control group were analyzed for statistical significance using two-tailed Student's t test: $^{**}P < 0.01$. (B) Induction of CYP3A4 mRNA expression in iPS cell–derived intestinal organoids: 40 μM rifampicin or 1 μM 1α,25-dihydroxyvitamin D_3 (VD3) was added in the last 72 hours. Total RNA was extracted, and mRNAs were analyzed using SYBR Green real-time PCR. Data are represented as mean ± S.D. (n = 3). mRNA expression levels were normalized relative to the mRNA level of HPRT. Gene expression levels are represented relative to the level in the control group, which was set to 1. Statistical significance of the differences compared with the control group was analyzed using two-tailed Dunnett's test: $^{*}P < 0.05$; $^{**}P < 0.01$. (C) Induction of metabolic activity of CYP3A4 in iPS cell–derived intestinal organoids: 40 μM rifampicin or 1 μM VD3 was added in the final 72 hours. Data are represented as mean ± S.D. (n = 4). The activity is represented relative to the level in the control group, which was set to 1. Differences relative to the control group were analyzed for statistical significance using two-tailed Dunnett's test: $^{*}P < 0.05$; $^{**}P < 0.01$.

intraluminal side of the intestinal organoids is on the side of the brush-border membrane. Moreover, the nonabsorbable marker FD-4 did not accumulate inside the organoids (Fig. 4, B and C), and ABCB1/MDR1- and ABCG2/BCRP-mediated transport was detected (Fig. 5, D–G; Supplemental Fig. 2). In recent years, studies to quantify the excretion function of ABCB1/MDR1 using three-dimensional intestinal organoids have been reported, and these organoids are expected to be applied as a P-glycoprotein inhibitor screening system (Mizutani et al., 2012; Zhang et al., 2016; Zhao et al., 2017). Because we successfully produced intestinal organoids with functional ABCB1/MDR1 transport from human iPS cells using A/PD/5-aza/DAPT, our intestinal organoids may be used in a drug development setting for such screening or for mechanistic studies to evaluate the contribution of ABCB1/MDR1 to intestinal transport and/or permeability. In addition to expressing diverse pharmacokinetic-related genes, the intestinal organoids exhibited CYP3A4 activity, and this activity was markedly inhibited by ketoconazole (Fig. 6A). CYP3A4 mRNA expression and activity were significantly upregulated by rifampicin and 1α,25-dihydroxyvitamin D_3 (Fig. 6, B and C), which are known to induce intestinal CYP3A4 through PXR and VDR, respectively (Thummel et al., 2001; Glaeser et al., 2005). Thus, the human iPS cell–derived intestinal organoids could potentially be useful for drug-development studies. However, in our intestinal organoids, the degrees of CYP3A4 mRNA induction and activity were less than those in other model systems, such as two-dimensional culture and animal models. Particularly, mRNA expression levels of PXR and VDR were low compared with those in adult small intestine (Supplemental Fig. 1, J and K). We suggest that the mRNA expression levels could be responsible for low CYP3A4 inducibility. To accurately evaluate pharmacokinetics in the small intestine, we need to develop a differentiation protocol that improves the metabolism and inducibility of CYP3A4 in our intestinal organoids. Here, we examined not only CYP3A4 but also other drug metabolism enzymes such as CYP2C9, 2C19, and 2D6, which are also expressed and involved in drug metabolism in the small intestine. These mRNA expression levels were similar to those in the small intestine (Supplemental Fig. 1, A–C). We suggest that it may be possible to also evaluate the first-pass metabolism involving phase I drug-metabolizing enzymes other than CYP3A4 in the intestinal organoids.

However, the inside of the organoids corresponds to the apical side of the small intestine, and this should be considered when assessing the process of drug absorption from the intestinal lumen. To examine the first-pass effects in the small intestine, new methods capable of evaluating the absorption process must be developed in future studies. For the evaluation of intestinal clearance, we need to clarify the correlation between in vivo systems and the intestinal organoids using various drugs for which a metabolic rate is already known and different. In addition, it would be necessary to quantitatively analyze the clearance with a mathematical modeling simulation technique. Thus, we plan to construct such a system in the future. For now, it is difficult to predict the intestinal clearance with the organoids; however, we believe it is possible to use the high-throughput screening system to judge whether the drugs are substrates or inducers of CYP3A4 and if the metabolites become inhibitors of metabolic enzymes or transporters.

Human iPS cell–derived intestinal organoids contained various cells that exist in the small intestine: enterocytes, intestinal stem cells, goblet cells, enteroendocrine cells, Paneth cells, and mesenchymal cells. Mesenchymal layers are critical for intestinal stem cell maintenance

and self-renewal (Yen and Wright, 2006), and mesenchymal layers have been reported to be involved in the fibrosis in Crohn's disease (Flier et al., 2010; Rieder et al., 2011). Because the human iPS cell–derived intestinal organoids include intestinal epithelial cells and mesenchymal layers, the organoids could be used as an in vitro model of human intestinal fibrosis.

In conclusion, we generated functional intestinal organoids from human iPS cells. These intestinal organoids not only expressed intestinal markers and pharmacokinetic-related genes but also exhibited ABCB1/MDR1 efflux transport activity, CYP3A4 activity and inducibility, and morphologic and functional features of the small intestine. Furthermore, we found that A/PD/5-aza/DAPT effectively induced the differentiation of human iPS cells into intestinal organoids. These intestinal organoids could be useful for drug development studies, including pharmacokinetic studies.

Acknowledgments

We thank Dr. Hidenori Akutsu, Dr. Yoshitaka Miyagawa, Dr. Hajime Okita, Dr. Nobutaka Kiyokawa, Dr. Masashi Toyoda, and Dr. Akihiro Umezawa for providing human iPS cells.

Authorship Contributions

Participated in research design: Onozato, Yamashita, Hashita, Iwao, Matsunaga.

Conducted experiments: Onozato, Yamashita, Akagawa, Kida, Nakanishi, Ogawa.

Performed data analysis: Onozato, Yamashita.

Wrote or contributed to the writing of the manuscript: Onozato, Yamashita, Hashita, Iwao, Matsunaga.

References

Barker N, van Es JH, Kuipers J, Kujala P, van den Born M, Cozijnsen M, Haegebarth A, Korving J, Begthel H, Peters PJ, et al. (2007) Identification of stem cells in small intestine and colon by marker gene *Lgr5*. *Nature* **449**:1003–1007.

Borlak J and Zwadlo C (2003) Expression of drug-metabolizing enzymes, nuclear transcription factors and ABC transporters in Caco-2 cells. *Xenobiotica* **33**:927–943.

Boudreau F, Rings EH, van Wering HM, Kim RK, Swain GP, Krasinski SD, Moffett J, Grand RJ, Suh ER, and Traber PG (2002) Hepatocyte nuclear factor-1α, GATA-4, and caudal related homeodomain protein Cdx2 interact functionally to modulate intestinal gene transcription. Implication for the developmental regulation of the sucrase-isomaltase gene. *J Biol Chem* **277**: 31909–31917.

Cetin Y, Müller-Köppel L, Aunis D, Bader MF, and Grube D (1989) Chromogranin A (CgA) in the gastro-entero-pancreatic (GEP) endocrine system. II. CgA in mammalian entero-endocrine cells. *Histochemistry* **92**:265–275.

Eglen RM and Randle DH (2015) Drug discovery goes three-dimensional: goodbye to flat high-throughput screening? *Assay Drug Dev Technol* **13**:262–265.

Finkbeiner SR, Freeman JJ, Wieck MM, El-Nachef W, Altheim CH, Tsai YH, Huang S, Dyal R, White ES, Grikscheit TC, et al. (2015) Generation of tissue-engineered small intestine using embryonic stem cell-derived human intestinal organoids. *Biol Open* **4**:1462–1472.

Flier SN, Tanjore H, Kokkotou EG, Sugimoto H, Zeisberg M, and Kalluri R (2010) Identification of epithelial to mesenchymal transition as a novel source of fibroblasts in intestinal fibrosis. *J Biol Chem* **285**:20202–20212.

Giacomini KM, Huang SM, Tweedie DJ, Benet LZ, Brouwer KL, Chu X, Dahlin A, Evers R, Fischer V, Hillgren KM, et al.; International Transporter Consortium (2010) Membrane transporters in drug development. *Nat Rev Drug Discov* **9**:215–236.

Glaeser H, Drescher S, Eichelbaum M, and Fromm MF (2005) Influence of rifampicin on the expression and function of human intestinal cytochrome P450 enzymes. *Br J Clin Pharmacol* **59**: 199–206.

González-Mariscal L, Betanzos A, Nava P, and Jaramillo BE (2003) Tight junction proteins. *Prog Biophys Mol Biol* **81**:1–44.

Gould SE, Junttila MR, and de Sauvage FJ (2015) Translational value of mouse models in oncology drug development. *Nat Med* **21**:431–439.

Hilgendorf C, Ahlin G, Seithel A, Artursson P, Ungell AL, and Karlsson J (2007) Expression of thirty-six drug transporter genes in human intestine, liver, kidney, and organotypic cell lines. *Drug Metab Dispos* **35**:1333–1340.

Iwao T, Kodama N, Kondo Y, Kabeya T, Nakamura K, Horikawa T, Niwa T, Kurose K, and Matsunaga T (2015) Generation of enterocyte-like cells with pharmacokinetic functions from human induced pluripotent stem cells using small-molecule compounds. *Drug Metab Dispos* **43**:603–610.

Kato M (2008) Intestinal first-pass metabolism of CYP3A4 substrates. *Drug Metab Pharmacokinet* **23**:87–94.

Liu F, Huang J, Ning B, Liu Z, Chen S, and Zhao W (2016) Drug discovery via human-derived stem cell organoids. *Front Pharmacol* **7**:334.

Martin P, Riley R, Back DJ, and Owen A (2008) Comparison of the induction profile for drug disposition proteins by typical nuclear receptor activators in human hepatic and intestinal cells. *Br J Pharmacol* **153**:805–819.

McCracken KW, Howell JC, Wells JM, and Spence JR (2011) Generating human intestinal tissue from pluripotent stem cells in vitro. *Nat Protoc* **6**:1920–1928.

Mizutani T, Nakamura T, Morikawa R, Fukuda M, Mochizuki W, Yamauchi Y, Nozaki K, Yui S, Nemoto Y, Nagaishi T, et al. (2012) Real-time analysis of P-glycoprotein-mediated drug transport across primary intestinal epithelium three-dimensionally cultured in vitro. *Biochem Biophys Res Commun* **419**:238–243.

Nakamura T, Sakaeda T, Ohmoto N, Tamura T, Aoyama N, Shirakawa T, Kamigaki T, Nakamura T, Kim KI, Kim SR, et al. (2002) Real-time quantitative polymerase chain reaction for MDR1, MRP1, MRP2, and CYP3A-mRNA levels in Caco-2 cell lines, human duodenal enterocytes, normal colorectal tissues, and colorectal adenocarcinomas. *Drug Metab Dispos* **30**:4–6.

Ogaki S, Shiraki N, Kume K, and Kume S (2013) Wnt and Notch signals guide embryonic stem cell differentiation into the intestinal lineages. *Stem Cells* **31**:1086–1096.

Paine MF, Hart HL, Ludington SS, Haining RL, Rettie AE, and Zeldin DC (2006) The human intestinal cytochrome P450 "pie". *Drug Metab Dispos* **34**:880–886.

Peeters T and Vantrappen G (1975) The Paneth cell: a source of intestinal lysozyme. *Gut* **16**: 553–558.

Perloff MD, Störmer E, von Moltke LL, and Greenblatt DJ (2003) Rapid assessment of P-glycoprotein inhibition and induction in vitro. *Pharm Res* **20**:1177–1183.

Reis CA, David L, Correa P, Carneiro F, de Bolós C, Garcia E, Mandel U, Clausen H, and Sobrinho-Simões M (1999) Intestinal metaplasia of human stomach displays distinct patterns of mucin (MUC1, MUC2, MUC5AC, and MUC6) expression. *Cancer Res* **59**:1003–1007.

Rieder F, Kessler SP, West GA, Bhilocha S, de la Motte C, Sadler TM, Gopalan B, Stylianou E, and Fiocchi C (2011) Inflammation-induced endothelial-to-mesenchymal transition: a novel mechanism of intestinal fibrosis. *Am J Pathol* **179**:2660–2673.

Robine S, Huet C, Moll R, Sahuquillo-Merino C, Coudrier E, Zweibaum A, and Louvard D (1985) Can villin be used to identify malignant and undifferentiated normal digestive epithelial cells? *Proc Natl Acad Sci USA* **82**:8488–8492.

Sander GR and Powell BC (2004) Expression of notch receptors and ligands in the adult gut. *J Histochem Cytochem* **52**:509–516.

Sato T, Stange DE, Ferrante M, Vries RG, van Es JH, van den Brink S, van Houdt WJ, Pronk A, van Gorp J, Siersema PD, et al. (2011) Long-term expansion of epithelial organoids from human colon, adenoma, adenocarcinoma, and Barrett's epithelium. *Gastroenterology* **141**:1762–1772.

Sato T, Vries RG, Snippert HJ, van de Wetering M, Barker N, Stange DE, van Es JH, Abo A, Kujala P, Peters PJ, et al. (2009) Single Lgr5 stem cells build crypt-villus structures in vitro without a mesenchymal niche. *Nature* **459**:262–265.

Sato Y, Shimamoto T, Amada S, Asada Y, and Hayashi T (2003) Large cell neuroendocrine carcinoma of the uterine cervix: a clinicopathological study of six cases. *Int J Gynecol Pathol* **22**: 226–230.

Shirasaka Y, Sakane T, and Yamashita S (2008) Effect of P-glycoprotein expression levels on the concentration-dependent permeability of drugs to the cell membrane. *J Pharm Sci* **97**:553–565.

Spence JR, Mayhew CN, Rankin SA, Kuhar MF, Vallance JE, Tolle K, Hoskins EE, Kalinichenko VV, Wells SI, Zorn AM, et al. (2011) Directed differentiation of human pluripotent stem cells into intestinal tissue in vitro. *Nature* **470**:105–109.

Sun D, Lennernas H, Welage LS, Barnett JL, Landowski CP, Foster D, Fleisher D, Lee KD, and Amidon GL (2002) Comparison of human duodenum and Caco-2 gene expression profiles for 12,000 gene sequences tags and correlation with permeability of 26 drugs. *Pharm Res* **19**: 1400–1416.

Takano M, Hasegawa R, Fukuda T, Yumoto R, Nagai J, and Murakami T (1998) Interaction with P-glycoprotein and transport of erythromycin, midazolam and ketoconazole in Caco-2 cells. *Eur J Pharmacol* **358**:289–294.

Tamminen K, Balboa D, Toivonen S, Pakarinen MP, Wiener Z, Alitalo K, and Otonkoski T (2015) Intestinal commitment and maturation of human pluripotent stem cells is independent of exogenous FGF4 and R-spondin1. *PLoS One* **10**:e0134551.

Thummel KE, Brimer C, Yasuda K, Thottassery J, Senn T, Lin Y, Ishizuka H, Kharasch E, Schuetz J, and Schuetz E (2001) Transcriptional control of intestinal cytochrome P-4503A by 1α,25-dihydroxy vitamin D_3. *Mol Pharmacol* **60**:1399–1406.

Watson CL, Mahe MM, Múnera J, Howell JC, Sundaram N, Poling HM, Schweitzer JI, Vallance JE, Mayhew CN, Sun Y, et al. (2014) An in vivo model of human small intestine using pluripotent stem cells. *Nat Med* **20**:1310–1314.

Yen TH and Wright NA (2006) The gastrointestinal tract stem cell niche. *Stem Cell Rev* **2**:203–212.

Zhang QY, Dunbar D, Ostrowska A, Zeisloft S, Yang J, and Kaminsky LS (1999) Characterization of human small intestinal cytochromes P-450. *Drug Metab Dispos* **27**:804–809.

Zhang Y, Zeng Z, Zhao J, Li D, Liu M, and Wang X (2016) Measurement of rhodamine 123 in three-dimensional organoids: a novel model for P-glycoprotein inhibitor screening. *Basic Clin Pharmacol Toxicol* **119**:349–352.

Zhao J, Zeng Z, Sun J, Zhang Y, Li D, Zhang X, Liu M, and Wang X (2017) A novel model of P-glycoprotein inhibitor screening using human small intestinal organoids. *Basic Clin Pharmacol Toxicol* **120**:250–255.

Address correspondence to: Dr. Takahiro Iwao, Department of Clinical Pharmacy, Graduate School of Pharmaceutical Sciences, Nagoya City University, 3-1 Tanabe-dori, Mizuho-ku, Nagoya 467-8603, Japan. E-mail: tiwao@phar.nagoya-cu.ac.jp

Generation of Intestinal Organoids Suitable for Pharmacokinetic Studies from Human Induced Pluripotent Stem Cells

Daichi Onozato, Misaki Yamashita, Anna Nakanishi, Takumi Akagawa, Yuriko Kida, Isamu Ogawa, Tadahiro Hashita, Takahiro Iwao, Tamihide Matsunaga

Department of Clinical Pharmacy, Graduate School of Pharmaceutical Sciences, Nagoya City University, Nagoya 467-8603, Japan. (D.O., M.Y., A.N., T.H., T.I., T.M.)

Educational Research Center for Clinical Pharmacy, Faculty of Pharmaceutical Sciences, Nagoya City University, Nagoya 467-8603, Japan. (T.A., Y.K., I.O, T.H., T.I., T.M.)

Drug Metabolism and Disposition

Supplemental Data

Supplemental Data 1. mRNA expression analysis of other pharmacokinetic-related genes.

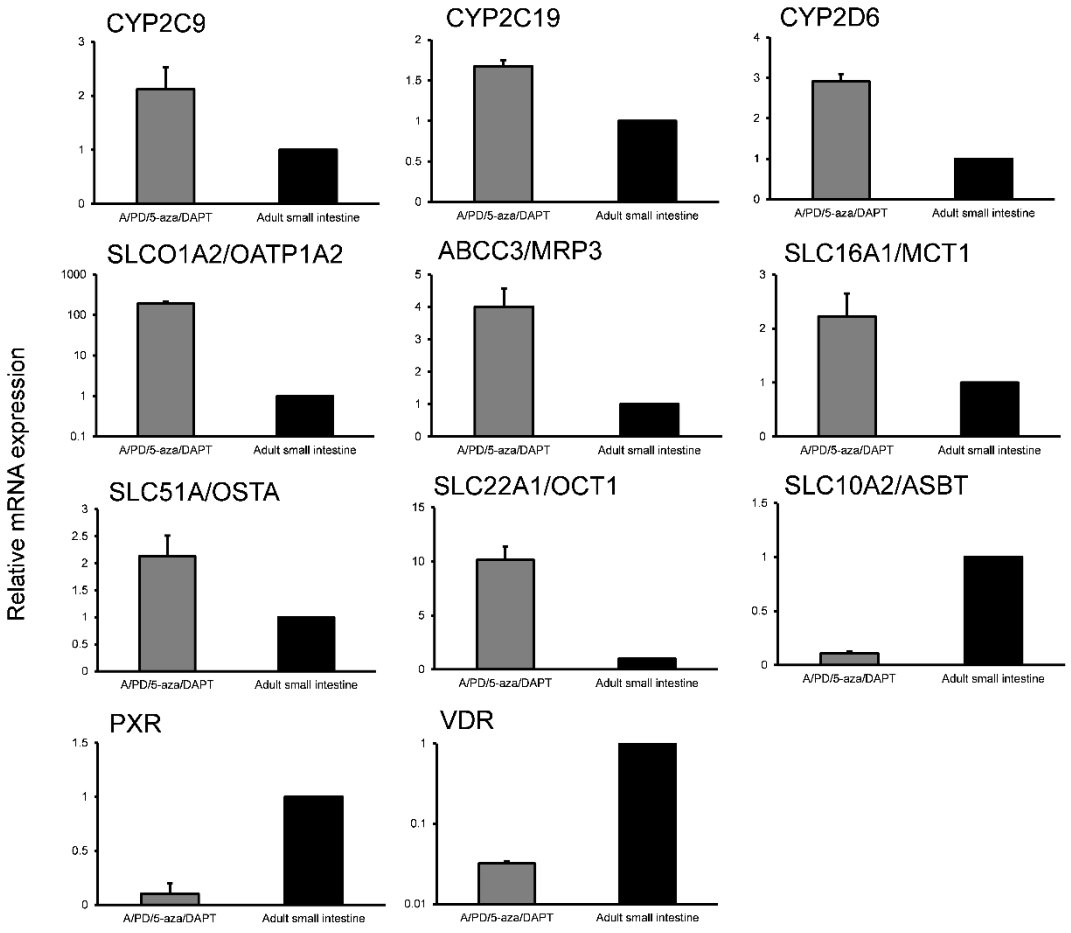

mRNA expression of other pharmacokinetic-related genes in human iPS cell-derived intestinal organoids using A-83-01/PD98059/5-aza-2′-deoxycytidine/DAPT (A/PD/5-aza/DAPT). After 34 days of differentiation, total RNA was extracted, and mRNAs were analyzed using SYBR Green real-time PCR. Data are represented as means ± S.D. (n = 3). All mRNA expression levels were normalized relative to the mRNA level of HPRT. Gene expression levels are represented relative to the level in adult small intestine, which was set to 1.

Supplemental Data 2. Hoechst33342 efflux transport analysis.

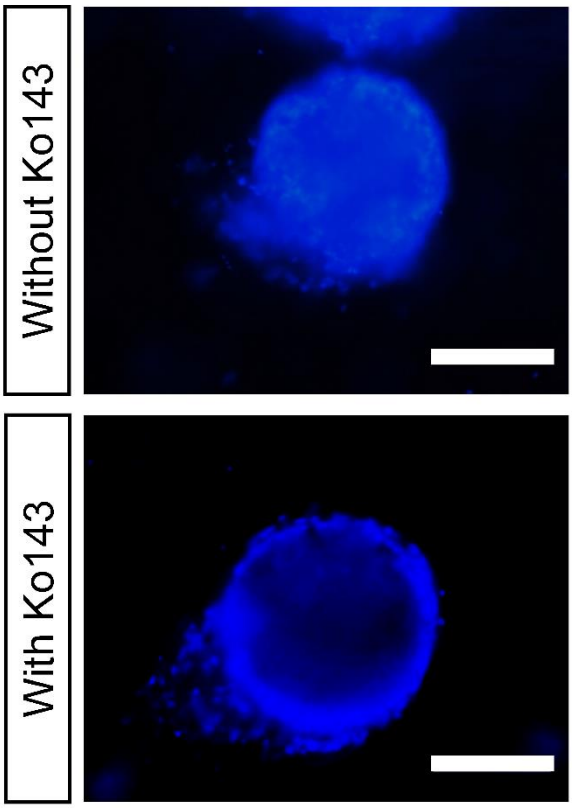

Efflux transport of hoechst33342 through ABCG2/BCRP. Organoids were incubated with hoechst33342 (10 μM) for 1 hour at 37°C in the absence or presence of Ko143 (100 μM). Scale bar, 100 μm.